A symmetry analysis of mechanisms in rotating rings of tetrahedra

By P.W. Fowler[1] and S.D. Guest[2]

[1]*Department of Chemistry, University of Exeter, Stocker Road, Exeter EX4 4QD, UK*
[2]*Department of Engineering, University of Cambridge, Trumpington Street, Cambridge CB2 1PZ, UK*

Rotating rings of tetrahedra are well known from recreational mathematics. Rings of N tetrahedra with N even are analyzed by symmetry-adapted versions of classical counting rules of mechanism analysis. For $N \geq 6$ a single state of self-stress is found, together with $N - 5$ symmetry-distinct mechanisms, which include the eponymous rotating mechanism. For $N = 4$ in a generic configuration, a single mechanism remains together with three states of self-stress, but uniquely in this case the mechanism path passes through a bifurcation at which the number of mechanisms and states of self-stress is raised by one.

Keywords: Symmetry; Mechanism; Mobility

1. Introduction

Rotating rings of tetrahedra are well known from recreational mathematics (Rouse Ball, 1939; Cundy and Rollet, 1981). An example is shown in Figure 1. These rings can be assembled from planar nets or by origami (Mitchell, 1997), and with recent 'microorigami' techniques have been constructed on a millimetre scale as prototypes for micro-fabrication in 3D (Brittain et al., 2001). The rings are often associated with decorations of the plane with various patterns and are also known as Kaleidocycles (Schattschneider and Walker, 1977; Schattschneider, 1977). The underlying mathematical objects are members of a family of cycles of edge-fused polyhedra having $2N$ vertices, $5N$ distinct edges, and $4N$ triangular faces where the faces are those of N edge-sharing tetrahedra, and where each tetrahedron in the cycle is linked to its predecessor and successor at opposite edges. Certain members of this family display an 'amusing and confusing' (Stalker, 1933) motion in which each tetrahedron of the toroidal ring turns, the whole turning inside out like a smoke-ring. The shared edges act as hinges between rigid tetrahedral bodies. Rotating rings of tetrahedra were described in a patent in 1933 (Stalker), but objects of this form occur in the earlier mathematical literature (Brückner, 1900). Animations of the motion are available at a number of sites on the world-wide web, e.g. Stark (2004).

Attention has centred on the case where the tetrahedra are equilateral, N is even, and N is greater than or equal to six. For $N = 8$ the motion is continuous, returning repeatedly to the starting configuration. For $N = 6$ the range of movement is restricted by clashes between faces, but the underlying motion can be

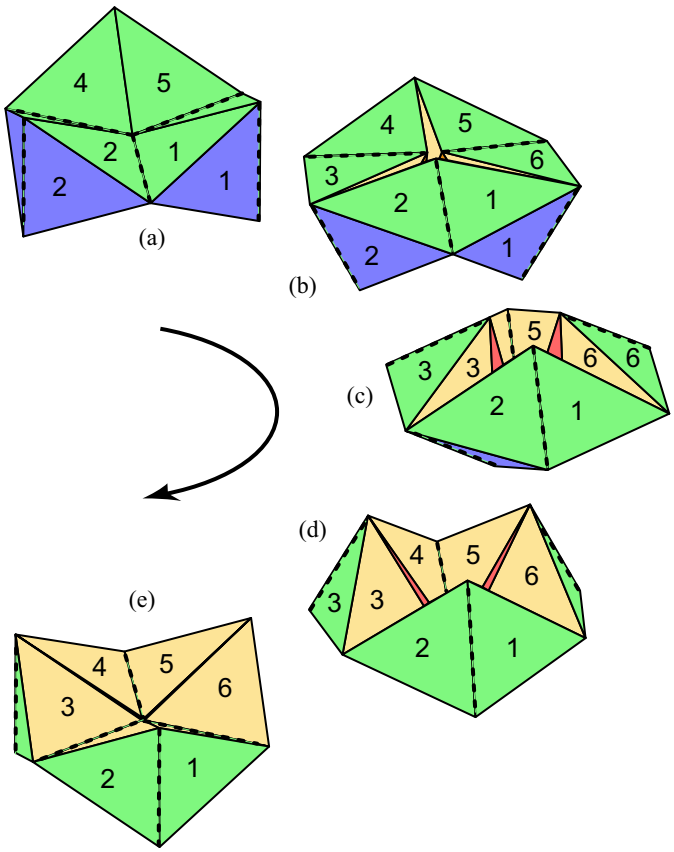

Figure 1. The finite motion of the rotating ring of six tetrahedra, showing one quarter of a complete cycle: (a) D_{3h} high symmetry point (the *standard* configuration); (b) generic C_{3v} symmetry; (c) D_{3d} high symmetry point; (d) generic C_{3v} symmetry; (e) D_{3h} high symmetry point. The tetrahedra are numbered, and the shared (hinge) edges between tetrahedra have been marked with a dashed line. Note that, in travelling from (a) to configuration (e), the structure has interchanged horizontal and vertical sets of shared (hinge) edges.

made continuous if the tetrahedra are transformed to an 'isosceles' shape by shrinking the shared edges; the system can be considered as a particular example of a 'threefold symmetric Bricard linkage' (Chen et al., 2005). The key feature common to equilateral and isosceles geometries is that successive shared edges remain mutually perpendicular. The present paper will concentrate on the cases of rings of N tetrahedra with this perpendicular hinge geometry and where N is even.

Our aim is to provide a general analysis of the mechanisms and states of self-stress in this subset of rotating rings of tetrahedra. For this purpose we use the recently developed symmetry-extended versions of the classical tools of mechanism analysis, the mobility criterion (Guest and Fowler, 2005) and the Maxwell counting rule (Fowler and Guest, 2000). The mobility criterion treats each tetrahedron as a rigid object, constrained by hinges along two opposite edges; Maxwell counting considers each tetrahedron to be formed from six spherically-jointed edge bars,

where two opposite bars are shared with neighbouring tetrahedra. Each description implies a relationship between the symmetries of mechanisms, states of self-stress and structural components; this approach takes full advantage of the high point-group symmetry of the even-N rings of tetrahedra.

Counting and symmetry analysis for toroidal frameworks has been considered before in the context of toroidal deltahedra (Fowler and Guest, 2002). There, it was shown that fully-triangulated toroids have at least six states of self-stress of well defined symmetry. Like the rotating rings, toroidal deltahedra have all triangular faces, but unlike the rings, the deltahedra are 'toroidal polyhedra' in that they enclose a single connected toroidal volume and all their edges are common to exactly two faces. The rotating rings, in which the enclosed tetrahedral volumes are disjoint and some edges are incident on four faces, are not polyhedral in this sense, and a different analysis is required.

2. Preliminary counting analysis

We begin with classical counting analyses, using both the mobility rule and the Maxwell count.

A generalised mobility rule is given in Guest and Fowler (2005) as

$$m - s = 6(N - 1) - 6g + \sum_{i=1}^{g} f_i \tag{2.1}$$

where m is the *mobility* (Hunt, 1978), or number of mechanisms, of a mechanical linkage consisting of N bodies connected by g joints, where each joint i permits f_i relative freedoms, and s is the number of independent states of self-stress that the linkage can sustain. The parameter s can be considered equivalently as the number of *overconstraints*, independent geometric incompatibilities, or misfits, that are possible for the linkage. In the present case, N is the number of tetrahedra, and there are $g = N$ hinge joints each permitting a single relative freedom, i.e., the revolute freedom between two adjacent tetrahedra. Thus,

$$m - s = N - 6. \tag{2.2}$$

The generalised Maxwell count for a system of spherically jointed bars is given by Calladine (1978) as

$$m - s = 3j - b - 6 \tag{2.3}$$

where j is the number of spherical joints and b is the number of bars connecting them. In the present case, $j = 2N$ and $b = 5N$, so that $m - s = N - 6$ from (2.3) in agreement with the mobility criterion (2.2).

As both m and s are non-negative integers, simple counting has therefore established the existence of at least one mechanism for $N > 6$, and conversely at least one state of self-stress for $N < 6$. From the counting result, the smallest ring of tetrahedra for which a mechanism *must* exist is that with $N = 7$, and indeed such a mechanism has been remarked in this case, and described as having 'an entire lack of symmetry' (Rouse Ball 1939).

For the case $N = 6$, counting alone does not demonstrate the existence of the known mechanism, but it does establish that if such a mechanism exists, then so must a state of self-stress.

In fact, a separate kinematic argument can be used to demonstrate that, in a generic configuration, $s = 1$ for all even $N \geq 6$. The argument runs as follows. Consider a ring in a *standard position* where the centres of the hinges define a planar N-gon, with $N/2$ of the hinges lying in the plane of the polygon, and the same number lying perpendicular to it. Cutting the ring along a single joint gives a chain of linked tetrahedra. This cut chain cannot sustain a state of self-stress: equilibrium of a terminal tetrahedron implies that the joint to the next tetrahedron in the chain is unstressed, and the same argument can be extended to the next in the chain, and so on for each of the other tetrahedra in turn. Thus any state of self-stress of the ring is contingent on restoration of the original joint, and is generated by a geometric misfit at the restored joint. Detailed consideration of the five possible misfits (corresponding to the five independent kinematic constraints imposed by a revolute joint) shows that four can be accommodated by rotation of the remaining $N - 1 \geq 5$ joints. The only type of misfit that cannot be so accommodated is *twisting*, and a misfit of this sort leads to a single 'twisting' state of self-stress. Hence $s = 1$ in the standard position. As the same argument can be advanced for nearby configurations, $s = 1$ in any *generic* configuration.

Given that $s = 1$, it follows from (2.2) shows that the number of mechanisms for even $N \geq 6$ is given by

$$m = N - 5. \tag{2.4}$$

Hence, the number of mechanisms grows linearly with N, although the counting approach gives no indication of the nature of these additional mechanisms; further insight into this aspect is given by considering the symmetry of the system.

3. Symmetry analysis: $N = 6$

This section will treat the case $N = 6$ in explicit detail, as a preliminary to a general analysis for all even N derived in section 4. The symmetry extension of the Maxwell counting rule is used; exactly equivalent results are given by the corresponding extension of the mobility rule.

The symmetry extension of Maxwell's rule (Fowler and Guest, 2000) is

$$\Gamma(m) - \Gamma(s) = \Gamma(j) \times \Gamma_T - \Gamma(b) - \Gamma_T - \Gamma_R \tag{3.1}$$

where $\Gamma(m)$, $\Gamma(s)$, $\Gamma(b)$ and $\Gamma(j)$, are the representations of the m mechanisms, s states of self-stress, b bars and j joints, and Γ_T, Γ_R are the translational and rotational representations (Atkins et al. 1970), all within the point group of the instantaneous configuration.

We will consider the ring of six tetrahedra in each of the three symmetry-distinct configurations that it can assume. In the standard position (Figure 1(a)), the six tetrahedra are arranged with D_{3h} point symmetry. The centres of the six hinges define a planar hexagon; hinges lie alternately in, and perpendicular to, this σ_h mirror plane. The normal through the centre of the hexagon defines the axis for the three-fold proper and improper rotations C_3 and S_3. A C_2 axis is defined by each horizontal hinge, and passes through the centre of the opposite, perpendicular, hinge. Each σ_v mirror plane contains one vertical, and one horizontal, hinge-line.

The Maxwell symmetry analysis can be laid out in tabular form as:

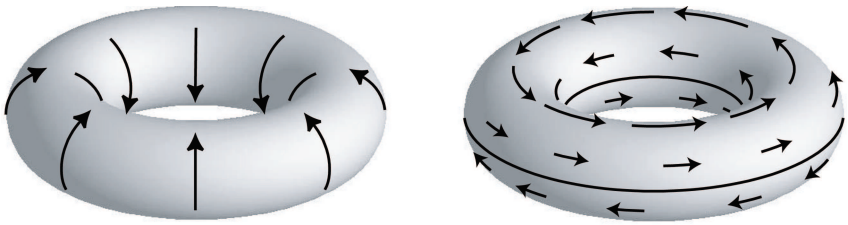

(a) (b)

Figure 2. Vector fields with the symmetry (a) Γ_z, and (b) Γ_ϵ on the torus. In D_{3h}, $\Gamma_z = A_2''$ and $\Gamma_\epsilon = A_1''$. Field (a) represents a motion by which inner and outer equators of the toroidal surface are exchanged, and by analogy with the pattern of current induced in a toroidal molecule by a rotating magnetic field, which gives rise to a molecular anapole moment (Ceulemans et al., 1998), can be called an 'anapole' rotation.

D_{3h}	E	$2C_3$	$3C_2$	σ_h	$2S_3$	$3\sigma_v$
$\Gamma(j)$	12	0	2	6	0	4
$\times\Gamma_T$	3	0	-1	1	-2	1
	36	0	-2	6	0	4
$-\Gamma_T - \Gamma_R$	-6	0	2	0	0	0
	30	0	0	6	0	4
$-\Gamma(b)$	-30	0	-2	-6	0	-2
$\Gamma(m) - \Gamma(s)$	0	0	-2	0	0	2

which reduces to

$$D_{3h} \qquad \Gamma(m) - \Gamma(s) = A_2'' - A_1'' \tag{3.2}$$

Hence symmetry analysis has predicted a mechanism of A_2'' symmetry, accompanied by a state of self-stress of A_1'' symmetry. A_2'' is the symmetry of the *anapole* rotation of a torus (Figure 2(a)) and describes the eponymous 'rotating' motion of this ring of tetrahedra. A_1'' is the symmetry of a *counter-rotating* pattern on a torus (Figure 2(b)) that describes the state of self-stress that would be generated by a twisting mismatch at each hinge.

If we displace the structure along the pathway of the A_2'' mechanism, the symmetry of the whole object falls to C_{3v}, with loss of C_2, σ_h and S_3 symmetry elements. In the reduced symmetry of this generic C_{3v} configuration (Figure 1(b)), the Maxwell calculation gives

$$C_{3v} \qquad \Gamma(m) - \Gamma(s) = A_1 - A_2. \tag{3.3}$$

This result can be verified by deleting columns in the tabular calculation above, or applying the 'descent in symmetry' correlation (Atkins et al. 1970)

$$A_1', \;\; A_2''\,(D_{3h}) \rightarrow A_1(C_{3v}),$$

$$A_2', \;\; A_1''\,(D_{3h}) \rightarrow A_2(C_{3v}).$$

In C_{3v} the mechanism is totally symmetric, and as there is no equisymmetric state of self-stress, the local linear analysis that we have carried out here is sufficient

to show that the mechanism for the ring of six tetrahedra is finite (Kangwai and Guest, 1999) i.e., even for finite displacements, there is a continuous mechanism path in the configuration space of the ring of tetrahedra.

If the finite mechanism is followed further along the displacement coordinate, the structure passes through a second point of high symmetry, a D_{3d} configuration (Figure 1(c)) where alternate hinges lie an equal angle above and below the horizontal plane. In this 'antiprism' configuration

D_{3d} $$\Gamma(m) - \Gamma(s) = A_{2u} - A_{1u}. \tag{3.4}$$

Continuation of the motion leads through C_{3v} configurations (Figure 1(d)) back to a D_{3h} position (Figure 1(e)) where horizontal and vertical hinges have been exchanged with respect to the initial setting. The cyclic nature of this finite mechanism is apparent.

Note that although its formulation across the three particular point groups uses different representation labels, the symmetry of the mobility excess for the ring of six tetrahedra is always compatible with the single expression,

$$\Gamma(m) - \Gamma(s) = \Gamma_z - \Gamma_\epsilon \tag{3.5}$$

where Γ_z is the symmetry of a translation along the principal axis, and Γ_ϵ is the representation of a pseudo-scalar (a quantity whose sign is preserved under proper, and reversed under improper operations). The mechanism is always an anapole rotation of an underlying torus, and the state of self-stress always follows a counter-rotating pattern on the torus, irrespective of the particular symmetry of the instantaneous configuration. Figure 2 shows how Γ_z and Γ_ϵ link to patterns of vectors on the torus.

To summarize, use of the Maxwell counting rule in its symmetry-adapted form has enabled us to give a complete account of the interesting static and kinematic behaviour for $N = 6$. Use of the symmetry-adapted mobility criterion (Guest & Fowler, 2005) gives the same results. This case has only one mechanism, the characteristic anapole rotation, but, as we have seen from pure counting, more mechanisms emerge for larger N. These too are amenable to a symmetry treatment, as the following section will demonstrate.

4. Symmetry analysis: the general case

The previous analysis can be generalised to cover all even values of N. Again we concentrate on Maxwell analysis, although all results reported here could also be obtained with the symmetry version of the mobility criterion. We consider the same sequence of standard $D_{(N/2)h}$, generic rotated $C_{(N/2)v}$, and alternate high-symmetry $D_{(N/2)d}$ antiprism configurations. For these groups we will use the notation $C(\phi)$ for the symmetry operation of rotation through ϕ about the principal axis, and $S(\phi)$ for the corresponding improper operation. $C(\phi)$ and $C(-\phi)$ belong to the same class, as do $S(\phi)$ and $S(-\phi)$. It turns out to be convenient to consider doubly odd cases, $N = 4p+2$, and doubly even cases, $N = 4p$, separately. The case $N = 4p$ is further split into $N = 4p$, $p > 1$ and $N = 4$, $p = 1$, as the standard notation for point groups C_{2v}, D_{2h}, D_{2d} ($p = 1$) differs from that for C_{2pv}, D_{2ph}, D_{2pd} ($p > 1$). In addition to this technicality the case $p = 1$ also presents some special features that justify a separate treatment, given in Section 5.

(*a*) *Rings with* $N = 4p + 2$

In the standard position, the N tetrahedra are arranged with $D_{(N/2)h} = D_{(2p+1)h}$ point symmetry. The centres of the hinges define a planar N-gon; hinges lie alternately within, and perpendicular to, the σ_h mirror plane. The normal through the centre of the hexagon defines the principal axis. A C_2' axis is defined by each horizontal hinge, and its opposite perpendicular partner; the same pair of hinges defines a σ_v mirror plane. The structure has $(2p + 1)$ C_2' axes, and $(2p + 1)$ σ_v planes.

The Maxwell symmetry analysis is:

$D_{(2p+1)h}$	E	$2C(\phi)$	$(2p+1)C_2'$	σ_h	$2S(\phi)$	$(2p+1)\sigma_v$
$\Gamma(j)$	$8p+4$	0	2	$4p+2$	0	4
$\times\Gamma_T$	3	c^+	-1	1	c^-	1
	$24p+12$	0	-2	$4p+2$	0	4
$-\Gamma_T-\Gamma_R$	-6	$-2c^+$	2	0	0	0
	$24p+6$	$-2c^+$	0	$4p+2$	0	4
$-\Gamma(b)$	$-20p-10$	0	-2	$-4p-2$	0	-2
$\Gamma(m)-\Gamma(s)$	$4p-4$	$-2c^+$	-2	0	0	2

where $c^\pm = \pm 1 + 2\cos\phi$. To reduce $\Gamma(m) - \Gamma(s)$ to a tractable form, we note that a representation Γ_Λ defined by

$$\Gamma_\Lambda = \Gamma(m) - \Gamma(s) + \Gamma_T + \Gamma_R - \Gamma_z + \Gamma_\epsilon \tag{4.1}$$

would have only integer characters

$D_{(2p+1)h}$	E	$2C(\phi)$	$(2p+1)C_2'$	$\sigma(h)$	$2S(\phi)$	$(2p+1)\sigma_v$
Γ_Λ	$4p+2$	0	-2	0	0	0

and specifically has a character under the identity that is equal to half the order of the point group. The structure of Γ_Λ is most easily understood by considering the limit $N \to \infty$, $D_{(2p+1)h} \to D_{\infty h}$. In $D_{\infty h}$, Γ_Λ reduces to an angular-momentum type expansion

$$\Gamma_\Lambda = \Sigma_g^- + \Sigma_u^+ + \Pi_g + \Pi_u + \Delta_g + \Delta_u + \Phi_g + \Phi_u + \ldots \tag{4.2}$$

with leading terms $\Gamma_T = \Sigma_u^+ + \Pi_u$, $\Gamma_R = \Sigma_g^- + \Pi_g$ followed by symmetries of scalar $(\Delta_g + \Phi_u + \ldots)$ and vector $(\Delta_u + \Phi_g + \ldots)$ cylindrical harmonics.

The symmetries in the series $\Pi_g + \Delta_g + \Phi_g + \ldots$ and $\Pi_u + \Delta_u + \Phi_u + \ldots$ are compactly written as E_{Lg} and E_{Lu} respectively, where $(L = 1) \equiv \Pi$, $(L = 2) \equiv \Delta$,... (Altmann and Herzig, 1994). Representations $E_{L(g/u)}$ are defined by their character under the operations of $D_{\infty h}$ as:

$D_{\infty h}$	E	$2C(\infty\phi)$	C_2	$\infty C_2'$	i	$2S(\infty\phi)$	$\sigma(h)$	$\infty\sigma_v$
E_{Lg}	2	$2\cos L\Phi$	$2(-1)^L$	0	2	$2(-1)^L\cos L\Phi$	$2(-1)^L$	0
E_{Lu}	2	$2\cos L\Phi$	$2(-1)^L$	0	-2	$-2(-1)^L\cos L\Phi$	$-2(-1)^L$	0

from which it is seen that the characters of E_{Lg} and E_{Lu} are equal under proper operations, and equal but opposite in sign under improper operations.

In the compact notation, (4.2) becomes

$D_{\infty h}$ $$\Gamma_\Lambda = A_{2g} + A_{1u} + \sum_{L=1}^{p}(E_{Lg} + E_{Lu}) \tag{4.3}$$

($\Sigma_g^- \equiv A_{2g}$, $\Sigma_u^+ \equiv A_{1u}$) which on descent back to $D_{(2p+1)h}$ is

$D_{(2p+1)h}$ $$\Gamma_\Lambda = A_2' + A_2'' + \sum_{L=1}^{p}(E_L' + E_L'') \tag{4.4}$$

which can be written as

$D_{(2p+1)h}$ $$\Gamma_\Lambda = \Gamma_T + \Gamma_R + \sum_{L=2}^{p}(E_L' + E_L'') \tag{4.5}$$

where $\Gamma_T = A_2'' + E_1'$, $\Gamma_R = A_2' + E_1''$, giving the final form of $\Gamma(m) - \Gamma(s)$ as

$D_{(2p+1)h}$ $$\Gamma(m) - \Gamma(s) = A_2'' - A_1'' + \sum_{L=2}^{p}(E_L' + E_L'') \tag{4.6}$$

where $A_2'' = \Gamma_z$ and $A_1'' = \Gamma_\epsilon$ in this group. Note that the result (4.6) reduces to (3.2) for D_{3h}, $N = 6$, $p = 1$, where the summation term would disappear.

Displacement along the Γ_z anapole mechanism takes the ring of tetrahedra to a $C_{(2p+1)v}$ point on the rotation pathway. The horizontal plane, C_2' axes and $S(\phi)$ improper axes are then no longer symmetry elements. The appropriate forms of equations (4.4) and (4.6) are

$C_{(2p+1)v}$ $$\Gamma_\Lambda = A_1 + A_2 + 2\sum_{L=1}^{p} E_L, \tag{4.7}$$

$C_{(2p+1)v}$ $$\Gamma(m) - \Gamma(s) = A_1 - A_2 + 2\sum_{L=2}^{p} E_L. \tag{4.8}$$

Again, the results for $N = 6$, $p = 1$ are recovered by deleting the summation terms.

At the intermediate 'antiprism' hinge configuration, the ring of tetrahedra has $D_{(2p+1)d}$ symmetry. In this point group, all perpendicular C_2' axes fall into a single class, each axis passing though the centres of opposite tetrahedra, and through the mid-points of four non-hinge bars. The σ_d mirror planes also constitute a single class, and each plane contains two opposite hinge bars. The equations (4.4) and (4.6) become

$D_{(2p+1)d}$ $$\Gamma_\Lambda = A_{2g} + A_{2u} + \sum_{L=1}^{p}(E_{Lg} + E_{Lu}), \tag{4.9}$$

$D_{(2p+1)d}$ $$\Gamma(m) - \Gamma(s) = A_{2u} - A_{1u} + \sum_{L=2}^{p}(E_{Lg} + E_{Lu}). \tag{4.10}$$

Again, the results for $N = 6$, $p = 1$ are recovered by deleting the summation terms.

(*b*) *Rings with $N = 4p$, $p > 1$*

In the standard position, the N tetrahedra are arranged with $D_{(N/2)h} = D_{(2p)h}$ point group symmetry. In $D_{(2p)h}$ there are two classes of binary rotation axis (C_2', C_2'') perpendicular to the principal axis, and two classes of reflection plane (σ_v, σ_d) that contain the principal axis. We choose C_2' to bisect two vertical hinges and C_2'' to contain two horizontal hinges. Consequently σ_v contains two vertical hinges, and σ_d contains two horizontal hinges.

The Maxwell symmetry calculation in tabular form is:

$D_{(2p)h}$	E	$2C(\phi)$	C_2	pC_2'	pC_2''	i	$2S(\phi)$	σ_h	$p\sigma_d$	$p\sigma_v$
$\Gamma(j)$	$8p$	0	0	0	4	0	0	$4p$	4	4
$\times\Gamma_T$	3	c^+	-1	-1	-1	-3	c^-	1	1	1
	$24p$	0	0	0	-4	0	0	$4p$	4	4
$-\Gamma_T - \Gamma_R$	-6	$-2c^+$	2	2	2	0	0	0	0	0
	$24p-6$	$-2c^+$	2	2	-2	0	0	$4p$	4	4
$-\Gamma(b)$	$-20p$	0	0	-2	-2	0	0	$-4p$	-2	-2
$\Gamma(m)-\Gamma(s)$	$4p-6$	$-2c^+$	2	0	-4	0	0	0	2	2

where again $c^\pm = \pm 1 + 2\cos\phi$. To reduce $\Gamma(m) - \Gamma(s)$, we again invoke Γ_Λ (4.1), which now has the integer characters

$D_{(2p)h}$	E	$2C(\phi)$	C_2	pC_2'	pC_2''	i	$2S(\phi)$	$\sigma(h)$	$p\sigma_d$	$p\sigma_v$
Γ_Λ	$4p$	0	0	0	-4	0	0	0	0	0

and again has the form of an angular momentum expansion in the $D_{\infty h}$ supergroup.

As there is no distinction between C_2' and C_2'' in $D_{\infty h}$, there is a subtlety in the termination of the expansion when N is doubly-odd: Γ_Λ is of order $4p$, and therefore can include only half of the four combinations comprised within the final pair of degenerate representations $E_{pg} + E_{pu}$. In $D_{(2p)h}$, $p > 1$, $E_{pg} + E_{pu}$ reduces to $B_{1g} + B_{2g} + B_{1u} + B_{2u}$ and inspection of characters under E and C_2'' shows that the half to be retained is $B_{1g} + B_{1u}$, the part of $E_{pg} + E_{pu}$ with character -1 under C_2''. Thus the form of Γ_Λ in $D_{(2p)h}$, $p > 1$ is

$$D_{(2p)h} \qquad \Gamma_\Lambda = A_{2g} + A_{2u} + B_{1g} + B_{1u} + \sum_{L=1}^{p-1}(E_{Lg} + E_{Lu}). \tag{4.11}$$

(Notice the change in labelling for $\Gamma_z = \Sigma_u^+$ on descent from $D_{\infty h}$ to $D_{(2p)h}$: in $D_{\infty h}$, the Altmann-Herzig convention is $\Gamma_z = A_{1u}$ but in $D_{(2p)h}$ with $1 < p < \infty$, $\Gamma_z = A_{2u}$.) From (4.11) Γ_Λ can be written for $p > 1$ as

$$D_{(2p)h} \qquad \Gamma_\Lambda = \Gamma_T + \Gamma_R + B_{1g} + B_{1u} + \sum_{L=2}^{p-1}(E_{Lg} + E_{Lu}) \tag{4.12}$$

and the final form of $\Gamma(m) - \Gamma(s)$ for $p > 1$ is then

$$D_{(2p)h} \qquad \Gamma(m) - \Gamma(s) = A_{2u} - A_{1u} + B_{1g} + B_{1u} + \sum_{L=2}^{p-1}(E_{Lg} + E_{Lu}), \tag{4.13}$$

where, as noted above, $A_{2u} = \Gamma_z$ and $A_{1u} = \Gamma_\epsilon$ in this group.

Displacement along the Γ_z anapole mechanism takes the ring of tetrahedra to a $C_{(2p)v}$ point on the rotation pathway. The horizontal plane, C_2' and C_2'' axes and $S(\phi)$ improper axes are then no longer symmetry elements. The appropriate forms of equations (4.11) and (4.13) are

$$C_{(2p)v} \qquad \Gamma_\Lambda = A_1 + A_2 + B_1 + B_2 + 2\sum_{L=1}^{p-1} E_L, \tag{4.14}$$

$$C_{(2p)v} \qquad \Gamma(m) - \Gamma(s) = A_1 - A_2 + B_1 + B_2 + 2\sum_{L=2}^{p-1} E_L. \tag{4.15}$$

Finally, at the intermediate 'antiprism' hinge configuration, the ring of tetrahedra has $D_{(2p+1)d}$ symmetry. In this point group, all perpendicular C_2' axes fall into a single class, each axis passing though the centres of opposite tetrahedra, and through the mid-points of four non-hinge bars. The σ_d mirror planes also constitute a single class, and each contains two opposite hinge bars. The equations (4.11) and (4.13) become

$$D_{(2p)d} \qquad \Gamma_\Lambda = A_2 + B_2 + \sum_{L=1}^{2p-1} E_L, \tag{4.16}$$

$$D_{(2p)d} \qquad \Gamma(m) - \Gamma(s) = B_2 - B_1 + \sum_{L=2}^{2p-2} E_L. \tag{4.17}$$

(*c*) *Interpretation*

We have derived explicit formulae for the mobility excess of rings of tetrahedra with doubly-odd and doubly-even N in each of three distinct symmetry groups. All six formulae (4.6, 4.8, 4.10, 4.13, 4.15, 4.17) can be subsumed in one general expression

$$\Gamma(m) - \Gamma(s) = \Gamma_z - \Gamma_\epsilon + (\Gamma_\Lambda - \Gamma_T - \Gamma_R) \tag{4.18}$$

where Γ_z is the non-degenerate representation of a one-parameter anapole mechanism transforming in the same way as simple translation along the main axis of the underlying torus, and Γ_ϵ is the non-degenerate representation of the unique state of self-stress. The final term $(\Gamma_\Lambda - \Gamma_T - \Gamma_R)$ includes contributions with negative weights, but as Γ_Λ contains complete copies of Γ_T and Γ_R for $N \geq 6$, the bracketed term is well defined: it is either vanishing ($N = 6$), or positive ($N > 6$).

Given that $(\Gamma_\Lambda - \Gamma_T - \Gamma_R)$ is a reducible representation with non-negative weights, and given the kinematic result $s = 1$, the mobility excess (4.18) resolves into separate expressions for the symmetries spanned by the states-of-self-stress and mechanisms:

$$\Gamma(s) = \Gamma_\epsilon, \tag{4.19}$$

$$\Gamma(m) = \Gamma_z + (\Gamma_\Lambda - \Gamma_T - \Gamma_R), \tag{4.20}$$

valid for generic configurations of rings with even $N \geq 6$.

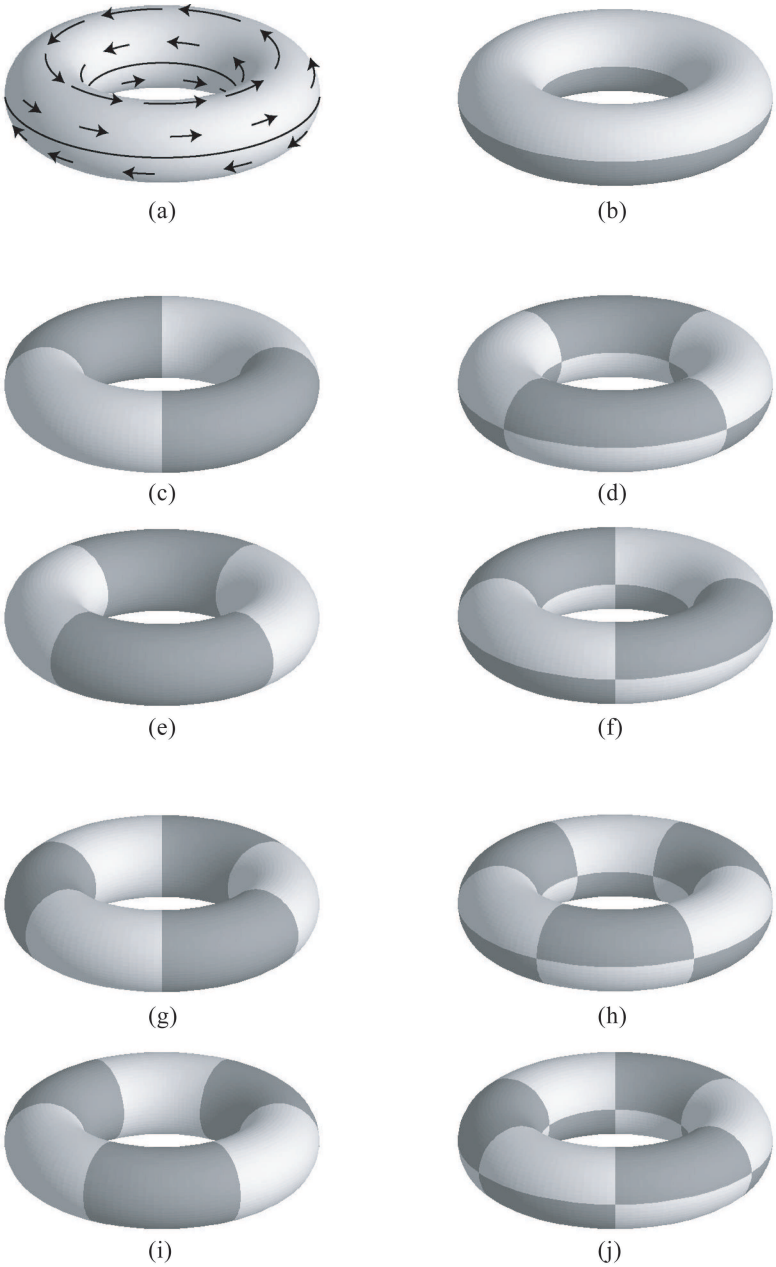

Figure 3. Representation of the single state of self-stress (a) and mechanisms (b)–(j), of rings of rotating tetrahedra, shown as decorations of a torus.
For $N = 6$: (a) shows A_2''; (b) shows A_1''.
For $N = 8$: (a) A_{1u}; (b) A_{2u}; (c) B_{1g}; (d) B_{1u}.
For $N = 10$: (a) A_2''; (b) A_1''; (c)&(e) E_2'; (d)&(f) E_2''.
For $N = 12$: (a) A_{1u}; (b) A_{2u}; (c)&(e) E_{2g}; (d)&(f) E_{2u}; (g) B_{1u}; (h) B_{1g}.
For $N = 14$: (a) A_2''; (b) A_1''; (c)&(e) E_2'; (d)&(f) E_2''; (g)&(i) E_3'; (h)&(j) E_3''.

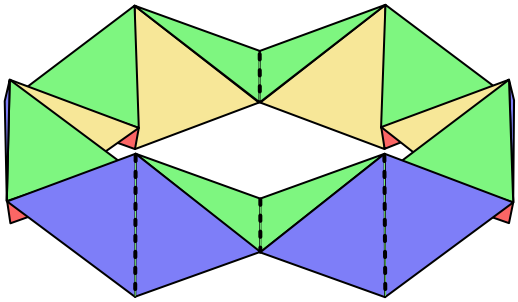

Figure 4. A ring of 12 tetrahedra in the standard setting. The faces of the tetrahedra have been shaded with the same colour scheme used in Figure1(a), and shared (hinge) edges between tetrahedra have been marked with a dashed line.

The angular-momentum description of Γ_Λ (4.3) gives a physical picture of the sets of mechanisms for $N > 6$ that are additional to the characteristic anapole rotation. As noted earlier, $(\Gamma_\Lambda - \Gamma_T - \Gamma_R)$ has terms of two types. In $D_{\infty h}$, the representations $E_{2g}, E_{3u}, E_{4g}, \ldots$ are those of scalar cylindrical harmonics, which can be visualised with appropriate patterns of shading on the torus (Figure 3, (c)&(e), (g)&(i)). A given $E_{n(g/u)}$ in this series describes a pair of functions that are interconverted on rotation of $\pi/2n$ about the main toroidal axis, each having n nodal planes containing that axis. Both members of the pair are symmetric with respect to reflection in the horizontal mirror plane. The alternate representations $E_{2u}, E_{3g}, E_{4u}, \ldots$ are those of vector cylindrical harmonics, and describe pairs of vector fields on the torus, again interconverting under rotation by $\pi/2n$, again having n nodal planes containing the vertical cylinder axis, but now antisymmetric with respect to reflection in the horizontal plane; each vector symmetry is related to a scalar harmonic symmetry through multiplication by Γ_z ($E_{ng} \times A_{1u} = E_{nu}$). The vector harmonics can also be visualised with appropriate shading of the torus (Figure 3, (d)&(f), (h)&(j)).

Physical models of the mechanisms of the ring of tetrahedra follow from the visualisations of Figure 3; for simplicity, we shall consider these in the standard setting. The case $N = 12$ is shown in the standard setting in Figure 4. The ring of N tetrahedra in the standard setting has $N/2$ vertical and $N/2$ horizontal hinges. A full description of the mechanisms is given if the freedoms of these two sets of hinges are treated separately, considering in turn one set to be locked and the other free to move.

Consider initially the case where the horizontal hinges are locked. The freedoms of a planar cycle of rigid bodies connected pairwise by $N/2$ perpendicular revolute hinges can be represented by sets of $N/2$ scalars (+ for opening, − for closing, say). If these scalars are considered using an angular momentum description (for $N = 12$ this is shown in Figure 5), then neither the concerted opening motion ($\Lambda = 0$) nor the pair of motions with a single vertical plane of antisymmetry ($\Lambda = 1$), correspond to mechanisms. The remainder of the $N/2$ independent combinations of hinge freedoms span exactly the series $E_{2g}, E_{3u}, E_{4g}, \ldots$ of the scalar cylindrical harmonics. When $N/2$ is even, the mechanisms occur in pairs; when $N/2$ is odd, one function at the highest value of Λ has nodes at all hinge positions and is dropped from the series.

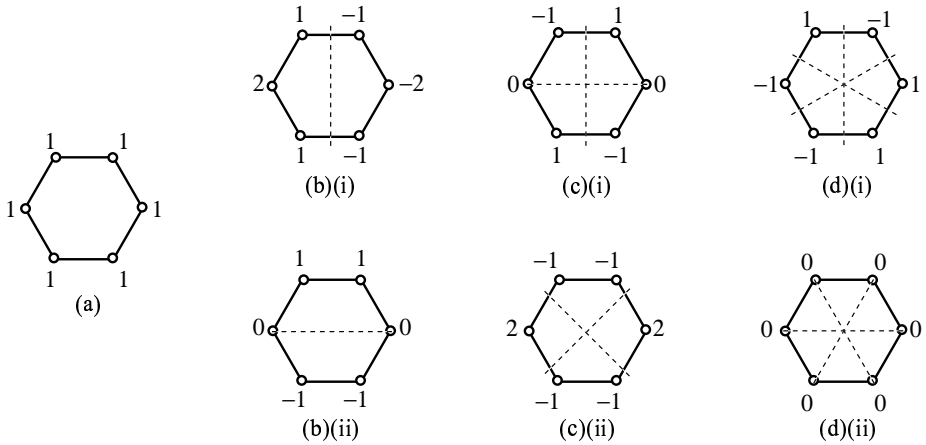

Figure 5. An angular momentum expansion of scalar values (not normalised) representing the opening or closing of the six vertical hinges in a ring of 12 tetrahedra. The bars between the vertical hinges correspond to pairs of tetrahedra joined by a locked horizontal hinge. (a) $\Lambda = 0$; (b) $\Lambda = 1$; (c) $\Lambda = 2$; (d) $\Lambda = 3$. The dashed lines show nodal planes. $\Lambda = 0$ and $\Lambda = 1$ do not correspond to mechanisms.

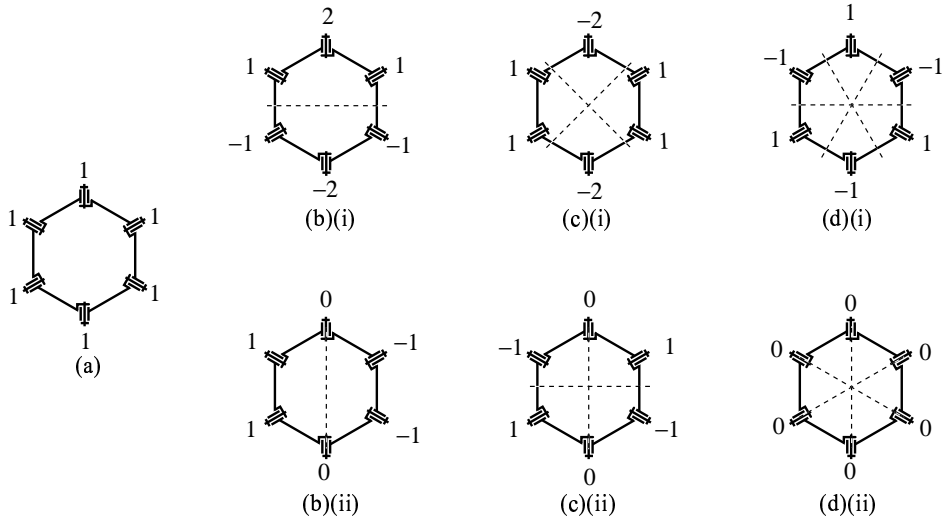

Figure 6. An angular momentum expansion of the vectors representing the opening or closing of the six horizontal hinges in a ring of 12 tetrahedra; each value is the magnitude of a vertical vector (not normalised). The bars between the horizontal hinges correspond to pairs of tetrahedra joined by a locked vertical hinge. (a) $\Lambda = 0$; (b) $\Lambda = 1$; (c) $\Lambda = 2$; (d) $\Lambda = 3$. The dashed lines show nodal planes. The pair $\Lambda = 1$ does not correspond to mechanisms; $\Lambda = 0$ is the anapole rotation.

Likewise, consider the case where the vertical hinges are locked. The freedoms of a planar cycle of rigid bodies connected pairwise by $N/2$ in-plane revolute hinges can be represented by sets of $N/2$ vectors normal to the cycle plane (+ phase in the half space of the hinge motion corresponding to approach of the connected bodies, say). If these vertical vectors are considered using an angular momentum description (for $N = 12$ this is shown in Figure 6) , the concerted motion of the hinges ($\Lambda = 0$) now corresponds to the anapole rotation of the ring of tetrahedra — instantaneously, at this configuration, the anapole mechanism requires rotations about only the horizontal hinges. The pair of motions with a single vertical plane of antisymmetry ($\Lambda = 1$) again do not correspond to mechanisms. The remainder of the $N/2$ independent combinations of hinge freedoms span exactly the series $E_{2u}, E_{3g}, E_{4u}, \ldots$ of the vector cylindrical harmonics. When $N/2$ is even, the mechanisms occur in pairs; when $N/2$ is odd, one function at the highest value of Λ has nodes at all hinge positions and is dropped from the series.

Once the ring of tetrahedra moves along any of the mechanisms, it loses the symmetry of the standard setting, and mechanisms may begin to mix in symmetry, with loss of the distinction between horizontal and perpendicular hinges, but the cylindrical harmonics still give a qualitative picture of the number and types of mechanism.

5. The special case $N = 4$

All of the analysis so far has been restricted to the rings of $N \geq 6$ tetrahedra. However, it is possible to assemble four suitably shaped tetrahedra in a ring. The steric constraints are severe, and in particular it is not possible to use physical regular tetrahedra, but for example right angled 'quarter-tetrahedra' formed by joining two opposite edge mid-points and two vertices of a regular tetrahedra are possible components. Much of the previous analysis applies in this case, although the equivalence of the symmetry results is obscured by differences in notation for abelian and non-abelian groups.

The case $N = 4$ has one obvious difference from the larger rings in that there is a bifurcation in the path followed by the mechanism. This is most clearly revealed by starting, not at the standard (in this case D_{2h}) configuration, but at the alternative high-symmetry point, the D_{2d} arrangement of four tetrahedra. Figure 7 shows the D_{2d} arrangement of four 'skinny' tetrahedra, and its equivalence to a set of four cubes. Figure 8 illustrates the bifurcation of the mechanism of the four-ring. Relative rotation (a) about one pair of collinear hinges leads from the D_{2d} configuration I, through a sequence of C_{2v} configurations (not shown) to the standard setting II; here the hinges have D_{2h} symmetry. Alternatively, relative rotation (b) about the other pair of collinear hinges leads to a distinct D_{2h} standard setting III. Each of the paths (a) and (b) are theoretically continuous, crossing at I, although when the ring is realised with the cubic blocks shown in the figure, steric clashes prevent continuation of the paths through the high symmetry point; this would not be the case with suitably skinny bodies. This is an example of a kinematotropic mechanism in the extended sense defined by Galletti and Fanghella (2001).

Counting (2.2) gives the mobility of the ring of four tetrahedra/cubes as $m - s = -2$. Symmetry analysis (3.1) gives the representation of the mobility in the different point groups accessed by the mechanisms as

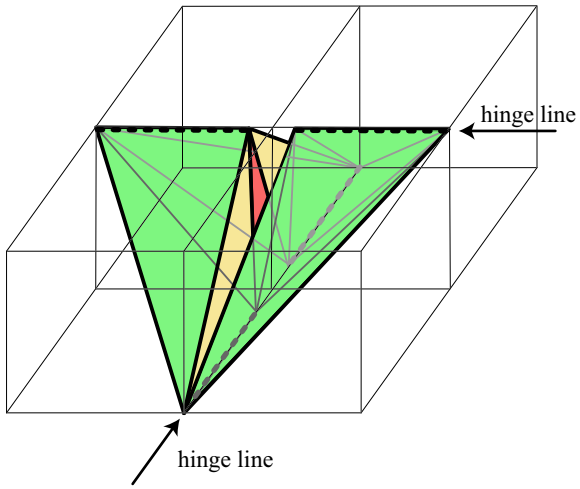

Figure 7. A ring of four tetrahedra in a D_{2d} configuration. The faces of the tetrahedra have been shaded with the same colour scheme used in Figure1(c), shared (hinge) edges between tetrahedra have been marked with a dashed line, and hidden lines are shown in grey. Fine lines show a set of four cubes hinged together in the same way that has equivalent mobility; the mechanisms are determined by the arrangement of hinge lines rather than the details of the hinged bodies.

$$D_{2d}(\mathrm{I}) \qquad \Gamma(m) - \Gamma(s) = B_2 - B_1 - E \tag{5.1}$$

$$C_{2v}(\mathrm{I}{\rightarrow}\mathrm{II}) \qquad \Gamma(m) - \Gamma(s) = A_1 - A_2 - B_1 - B_2 \tag{5.2}$$

$$D_{2h}(\mathrm{II}) \qquad \Gamma(m) - \Gamma(s) = B_{1u} - B_{3g} - A_u - B_{3u} \tag{5.3}$$

$$C_{2v}(\mathrm{I}{\rightarrow}\mathrm{III}) \qquad \Gamma(m) - \Gamma(s) = A_1 - A_2 - B_1 - B_2 \tag{5.4}$$

$$D_{2h}(\mathrm{III}) \qquad \Gamma(m) - \Gamma(s) = B_{1u} - B_{2g} - A_u - B_{2u} \tag{5.5}$$

The symmetry analysis in all configurations shows a single mechanism and three states of self-stress. Analysis in the generic C_{2v} configuration along one of the two branches shows a totally symmetric mechanism with no blocking equisymmetric state of self-stress; the mechanism is therefore finite (Kangwai and Guest, 1999).

Neither the counting nor symmetry analysis gives any hint of the presence of a second mechanism at the D_{2d} bifurcation point. Indeed this a clearly a geometric phenomenon, critically dependent on the simultaneous collinearity of two pairs of hinges at this configuration. This is compatible with, but not implied by D_{2d} symmetry; mechanisms which require special geometric configurations will always escape a generic symmetry analysis, and require a specific analysis at the special geometry. A structure in which the meeting points of the collinear pairs were symmetrically displaced along the z axis, leaving the outer ends of the hinges unshifted, would still belong to the D_{2d} point-group, but only the single mechanism predicted by the symmetry mobility analysis would remain; such a system however would not be a ring of tetrahedra in the strict sense defined in Section 1

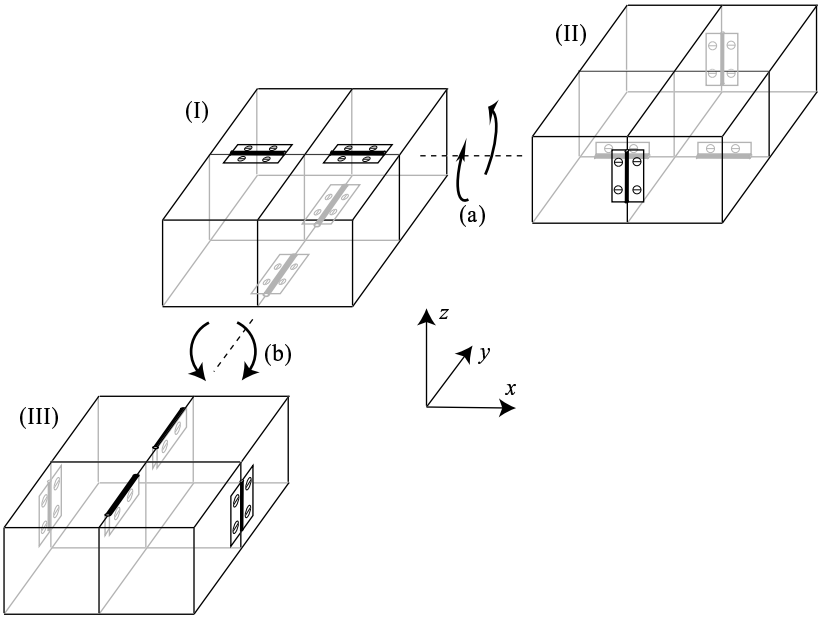

Figure 8. A set of four hinged cubes used to show the mobility of a ring of four tetrahedra: the relationship between the four cubes and the four tetrahedra is shown in Figure 7. I shows the D_{2d} bifurcation configuration: two mechanism paths emerge. Relative rotation (a) about one pair of collinear hinges leads from the D_{2d} configuration I, through a sequence of C_{2v} configurations (not shown) to the standard setting II; here the hinges have D_{2h} symmetry. Alternatively, relative rotation (b) about the other pair of collinear hinges leads to a distinct D_{2h} standard setting III.

6. Conclusions

This paper provides a general symmetry analysis of a ring of even-N regular tetrahedra. Symmetry reveals that generically, for even $N \geq 6$, the count $m - s = N - 6$ comes from $s = 1$ states of self-stress, and a symmetrically distinct $m = N - 5$ mechanisms. The finite nature of these mechanisms is also shown, including the eponymous 'rotating' mechanisms. The treatment shows the utility of a symmetry analysis in enriching the information available from pure counting.

The $N = 4$ case has been considered separately. Here, generically, symmetry shows that the count $m - s = N - 6$ comes from $s = 3$ states of self-stress, and $m = 1$ mechanisms. Uniquely in this case the 'rotating' mechanism passes through a particular geometric configuration where there is a bifurcation in the mechanism path. Detection of the bifurcation is outside the symmetry classification.

The analysis as presented considers only even-N cases that lie on the path followed by the rotating mechanism. For $N > 6$, there are many other mechanism paths, leading to lower symmetry configurations, and other points of mechanism bifurcation, that could be followed; we have not considered these other paths, although the general methodology remains valid for them.

It is possible to generalise the even-N ring of tetrahedra with mutually perpendicular hinges that is considered in this paper. Odd-N rings can be constructed.

The case $N = 7$ was noted by Coxeter (Rouse Ball, 1939), and we have constructed an example using skinny tetrahedra. Generically it has C_1 symmetry (no symmetry operation other than the identity), but passes though two distinct C_2 high-symmetry configurations; in the generic C_1 configuration, symmetry analysis reduces to simple counting.

The objects considered here all have a cylindrical topology: if a path around the ring is followed, passing from one tetrahedron to the next along faces that are adjacent, either across an edge or a vertex, then eventually the face that was the initial starting point is reached. For skinny tetrahedra, it is also possible to join even-N rings with a Mobius twist (Stark, 2004). We have constructed examples of rings of tetrahedra with mutually perpendicular hinges that have a Mobius twist, but found that accessible symmetries, at least for $N = 8$, are rather low.

Finally, recent investigations (Gan & Pellegrino, 2003; Chen et al., 2005) have shown that the mobility of rings may persist under relaxation of the condition that consecutive hinges are perpendicular. Many of these systems have potential application as deployable structures.

SDG acknowledges the support of the Leverhulme Trust.

References

Altmann, S. L. and Herzig, P. 1994 *Point-group theory tables.* Oxford: Clarendon Press.

Atkins, P. W., Child, M. S. & Phillips, C. S. G. 1970 *Tables for Group Theory.* Oxford: Clarendon Press.

Brittain, S. T., Schueller, O. J. A., Wu, H., Whitesides, S. & Whitesides, G. M. 2001 Micro-origami: Fabrication of small, three-dimensional, metallic structures. *J. Phys. Chem. B* **105**, 347–350.

Brückner, M. 1900 *Vielecke und Vielflache.* Leipzig: B.G. Teubner.

Chen, Y., You, Z. and Tarnai, T. 2005 Threefold-symmetric Bricard linkages for deployable structures. *Int. J. Solids Struct.* In press, doi:10.1016/j.ijsolstr.2004.09.014.

Calladine, C.R. 1978 Buckminster Fuller's 'Tensegrity' structures and Clerk Maxwell's rules for the construction of stiff frames, *Int. J. Solids Struct.* **14**, 161–172.

Ceulemans, A., Chibotaru, L.F. and Fowler, P.W. 1998 *Phys. Rev. Lett.* **80**, 1861–1864.

Cundy, H. M. & Rollett, A. R. 1939 *Mathematical Models, 3rd edition.* Tarquin Publications.

Fowler, P. W. & Guest, S. D. 2002 Symmetry and states of self stress in triangulated toroidal frames. *Int. J. Solids Struct.* **39**, 4385–4393.

Fowler, P. W. & Guest, S. D. 2000 A symmetry extension of Maxwell's rule for rigidity of frames. *Int. J. Solids Struct.* **37**, 1793–1804.

Galleti, C. & Fanghella, P. 2001 Single-loop kinematotropic mechanisms. *Mech. Mach. Theory* **36**, 743–761.

Gan, W. W. & Pellegrino, S. 2003 Closed-Loop Deployable Structures. In *Proc. 44th AIAA/ASME/ASCE/AHS/ASC Structures, Structural Dynamics and Materials Conference, 7-10 April 2003, Norfolk, VA* AIAA 2003-1450.

Guest, S. D. & Fowler, P. W. 2005 A symmetry-extended mobility rule. Accepted for publication in *Mech. Mach. Theory.*

Hunt, K. H. 1978 *Kinematic Geometry of Mechanisms.* Oxford: Clarendon Press.

Kangwai, R. D. & Guest, S. D. 1999 Detection of finite mechanisms in symmetric structures. *Int. J. Solids Struct.* **36**, 5507–5527.

Mitchell, D. 1997 *Mathematical Origami: Geometrical Shapes by Paper Folding.* Tarquin Publications.

Rouse Ball, W. W. 1939 *Mathematical Recreations and Essays, 11th edition.* Revised and extended by Coxeter, H.S.M. London: Macmillan and Co., Ltd.

Schattschneider, D. 1988 Creating kaleidocycles and more. In *Shaping Space. A Polyhedral Approach* ed. Senechal M. & Fleck G. Basel: Birkhuser, pp. 57–60.

Schattschneider, D. and Walker, W. 1977 *M.C. Escher Kaleidocycles* New York: Ballantine Books. Editions are available in 17 languages, including: *M.C.Escher Kaleidozyklen* Cologne: Taschen, 1992 *M.C. Escher Kalejdocykler* Berlin: Taschen, 1990. *M.C. Escher Caleidocycli* Cologne: Evergreen, 1992.

Stark, M. 2004 *the kaleidohedron from the IsoAxis grid* http://www.ac-noumea.nc/maths/amc/polyhedr/IsoAxis_.htm. (dated February 2000, updated 28-07-2004)

Stalker, R.M. 1933 *Advertising medium or toy.* US Patent 1,997,022, filed April 27, 1933, and issued April 9, 1935.